PCCP

Accepted Manuscript

ROYAL SOCIETY OF CHEMISTRY

www.rsc.org/pccp

Resistive switching memory devices based on electrical conductance tuning in poly (4-vinyl phenol)-oxadiazole composites

Yanmei Sun[a], Fengjuan Miao[a], Rui Li[b]

a Communication and Electronics Engineering Institute, Qiqihar University, Qiqihar 161006, China

b Department of Physics, College of Science, Qiqihar University, Qiqihar 161006, China

ABSTRACT Nonvolatile memory devices, based on electrical conductance tuning in thin films of poly (4-vinyl phenol) (PVP) and 2-(4-tert-butylphenyl)-5-(4-biphenylyl)-1, 3, 4-oxadiazole (PBD) composites, are fabricated. The current-voltage characteristics of the fabricated device show different electrical conductance behaviors, such as write-once read-many-times (WORM) memory effect, rewritable flash memory effect and insulator behavior, which depend on the content of PBD in the PVP+PBD composites. The OFF and ON states of the WORM and rewritable flash memory devices are stable under a constant voltage stress or a continuous pulse voltage stress at a read voltage. The memory mechanism is deduced from the modeling of the nature of currents in both states in the devices.

KEYWORDS: Poly (4-vinyl phenol), PBD, flash, memory, conductance switching

1. Introduction

The intense activity in the study of resistive organic memories is motivated by their extremely simple structure and ability for scaling to small dimensions.[1,2] Such devices can also be stacked in multiple levels, providing 3-D architectures.[3] Among the reported materials for resistor memories,[4-19] polymer blend materials have significant advantages compared to others due to their easy and diverse modulation of the host polymers and guest additives to control the resulted memory characteristics.[4-6] Typical guest additives can be embedded within polymers such as metal nanoparticles,[7, 8] graphitic carbon-based nanomaterials (graphene,[9 - 11] fullerenes,[6, 12] and nanotubes,[13,14]), organic polymer molecules,[15, 16] and small molecules.[17-19] The polymers serve as an electrically functional host or just a supporting matrix, whereas the guest additives have an interaction with polymers or among themselves. The distribution and concentration of the addition in the blend system play a significant role in the reversibility or volatility of electronic resistance observed in the thin film state under the applied external electrical stress.

It is generally known that good electron-transporting materials used in organic electronic devices can effectively improve device performances. Oxadiazole derivatives were widely reported as ideal electron-transporting materials in organic electronic devices.[20-26] 2-(4-tert-butylphenyl)-5-(4-biphenylyl)-1, 3, 4-oxadiazole (PBD) is one of the most efficient electron-transporting materials due to its high electron affinity. Nevertheless, thin films of such low molar mass oxadiazoles are usually prepared by vacuum evaporation. Although the films are amorphous, they have a strong tendency to crystallize.[27] One simple alternative to low molecular weight compounds

is guest-host systems in which the small molecular compounds are embedded in a polymer matrix-like PVK and PU.[28,29]

In previous work, we have reported on bistable electrical switching and nonvolatile memory effect in PBD blending with PVK and PU.[28,29] Our results indicate that the devices based on PBD and PVK composites demonstrate extremely steady performance due to the strong interaction between acceptor and donor, and the addition of PBD in PU film showed a marked increase in ON/OFF current ratio and a obvious expansion in memory window. In our previous work, the influence of blending level on memory behaviors of organic film focused mostly on stability of the performance or ON/OFF state current ratio. The blending level does not play a significant part in determining the memory type of the guest-host systems, despite it shows an important influence on the performances of device. However, in the present work, we have found that the memory devices based on the poly (4-vinyl phenol) and PBD composite materials exhibit different memory types with the blending level changing. Therefore, systematic studies on the effects of oxadiazole derivatives on the electrical properties of the organic memory devices are still necessary to enhance device efficiency, and some key factors that affect the switching and memory capability of polymer blend materials still remain to be resolved.

In this work, we report the controllable electrical conductance switching and nonvolatile memory effects in PVP and PBD composite thin films. The electrical and bistable switching behaviors of the PVP+PBD composite films can be tuned by varying the PBD content (blending level) in the composite films. Bistable electrical conductance switching behaviors, including (i) rewritable flash memory effects, (ii) write-once read-many-times (WORM) memory effects, and (iii) insulator behavior, can be realized in an ITO/PVP+PBD/Al sandwich structure by increasing the PBD content in the PVP+PBD composite film.

2. Experimental Section

PVP (average M_w=25000) and PBD (M_w=354) were both provided by Sigma-Aldrich. The chemical structures of the compounds used in this study, PVP and PBD are shown in Fig. 1(a). The indium tin oxide (ITO) conductive glasses of dimensions 2 cm×1 cm (sheet resistance $R_{\square}$ =6-9 Ω/□) were precleaned sequentially with deionized water, acetone, isopropanol and methanol by ultrasonication for 20 min and then dried in a vacuum oven at 70 ℃ for 6 h. The sandwich memory devices using the mixture of PVP and PBD as the active layer with different mixture ratio were fabricated by spreading a 35 mg/ml solution of mixture of PVP and PBD, in mixed solvents of 2:1 (volume ratio) ethanol and *N*-methyl-2-pyrrolidone onto a ITO substrate using a spin coater set at 900 rpm for 18 s, and then 3000 rpm for 60 s. The spin-coated mixture films were then baked at 60 ℃ for 8 h under vacuum of 100 Pa to remove the residual solvent. Finally, the sandwich

devices were fabricated by vacuum evaporation of a thin Al layer at a pressure of 1.0×10^{-4} Pa under a uniform deposition rate of 3-5 Å/s with a thickness of 200 nm through a shadow mask onto the mixture surface as the top electrode. The architecture of the ITO/PVP+PBD/Al structures investigated in this work is depicted in Fig. 1(b). The electrical characterization of the memory device was performed by a Keithley 4200-SCS semiconductor parameter analyzer equipped with a Keithely 4205-PG2 arbitrary waveform pulse generator. ITO was grounded during all voltage scans with a step of 0.05 V. In order to prevent breakdown of the memory devices when voltages were applied on the devices, a compliance current of 0.1 A was set.

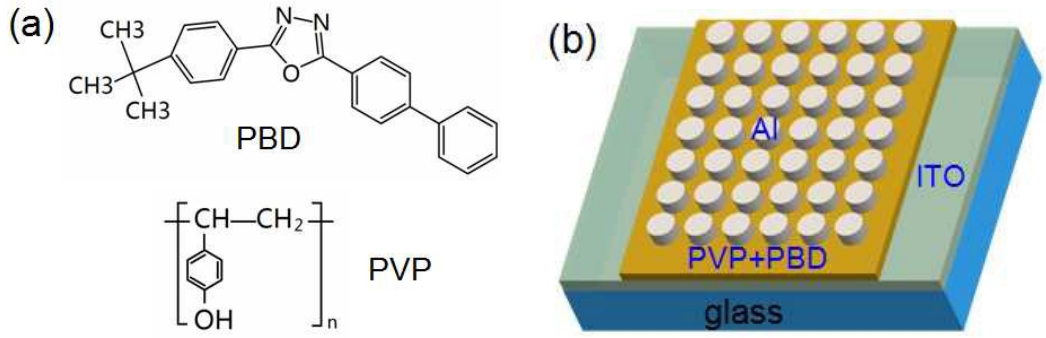

Fig. 1 (a) Chemical structures of PBD and PVP. (b) Schematic of the ITO/PVP+PBD/Al sandwich device

3. Results and Discussion

The conductance switching and memory effects of PVP+PBD composites are demonstrated by the current-voltage (*I-V*) characteristics of the ITO/PVP+PBD/Al sandwich devices. Before investigation of the memory effects of the blends, we first measured the devices' electrical performance of the single component with the active material PVP insulating polymer sandwiched between the ITO and Al electrodes. As shown in Fig. 2(a), the device switches from the low conductivity (OFF) state to the high conductivity (ON) state at about -1.30 V when the voltage applied is increased from 0 to -4.0 V (sweep 1 in Fig. 2(a)). In the subsequent sweep (sweep 2), the device remains in its high conductivity state. Once the positive bias was swept from 0 to 6 V (sweep 3), high conductivity state was kept until the bias exceeded the threshold voltage (3.75 V) and low conductivity state was recovered. When the bias was swept from 0 to 6 V once again (sweep 4), the devices were remained in OFF state. The devices showed a current ON/OFF ratio of about 313-980 for voltage in the range of -4 to 6 V, as shown in Fig. 2(b). Hence, the memory device exhibits a typical nonvolatile flash memory characteristic.

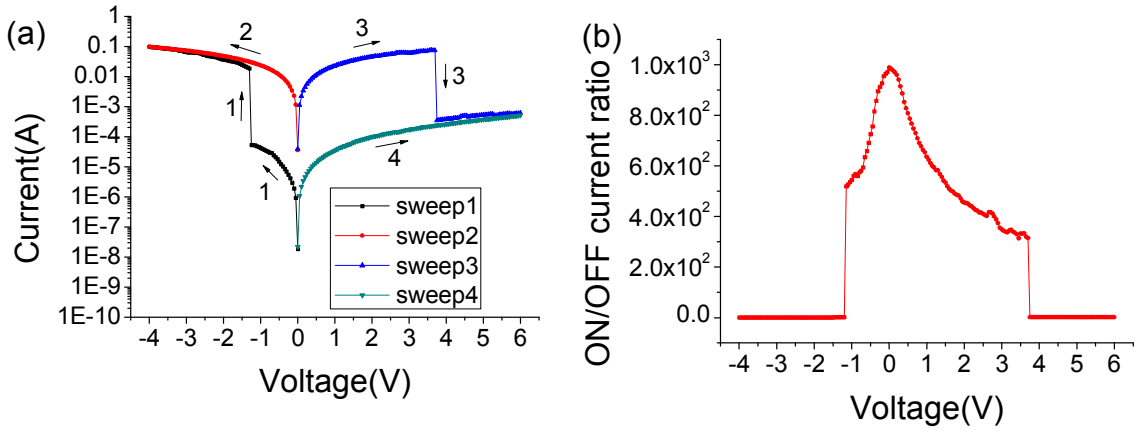

Fig. 2 (a) *I-V* characteristics of the ITO/PVP/Al memory devices. (b) Relationship between the ON/OFF current ratio and the applied voltage in the above device.

Fig. 3(a) presents the *I-V* characteristics for blends-based memory device with 5 wt. % PBD. It exhibits similar nonvolatile flash switching behavior. This device initially exhibited a low conductivity (OFF) state with the lower OFF state current comparable with the ITO/PVP/Al devices. As the negative sweep voltage increased to the threshold voltage of -1.4 V, the current changed abruptly from 10^{-6} to 10^{-2} A (sweep 1), switching the device from the low conductivity (OFF) state to the high conductivity (ON) state. The transition from the OFF to ON states is equivalent to the "writing" process in a digital memory. After the transition was achieved, the device remained in this ON state during the subsequent scan from 0 to -4 V (sweep 2). The ON state could be programmed back to the initial OFF state by a positively biased sweep with sufficient magnitude of 3.55 V (sweep 3). This is equivalent to the "erasing" process. The device remained in this OFF state during the subsequent scan from 0 to 6 V (sweep 4), thus completing the "write-read-erase-read" (WRER) cycle for a nonvolatile rewritable memory device. The above processes can be repeated many times for individual memory cells. In the case of the device with 5 wt. % PBD, a higher ON/OFF state current ratio of about 5×10^{3}-1.4×10^{4} in the range of -4 to 6 V is shown in Fig. 3(b). No significant degradation of the device in both the ON and OFF states was observed after 9.4 h of the continuous stress test (Fig. 3(c)), indicating that the composite materials are stable. The ON/OFF state current ratio in the bistable devices is high enough to promise a low misreading rate through the precise control of the ON and OFF states. The effect of continuous read pulses (with a read voltage of 2 V) on the ON and OFF states is also investigated. As shown in Fig. 3(d), more than 300 read cycles are conducted on the ITO/PVP+PBD/Al devices and no increase in resistance (degradation in current) is observed for the ON and OFF states. Neither the voltage stress nor the read pulses cause state transition because the applied voltage (2 V) is lower than the switching threshold voltage. Thus, both states are stable under voltage stress and are insensitive to read pulses. Fig. 3(e) shows the cyclic voltage stress at -3 V for writing, -1 V for

reading, 5 V for erasing and 2 V for rereading from 1 to 160 cycles for containing 5 wt. % PBD blend device. The devices exhibit a highly stable characteristic with well-resolved states in terms of operating repeated WRER sequence test. In all cases, the high conductivity state can be restored to the low conductivity state successfully. The highly controllable resistance modulation of the blend device implies that the conducting pathway is repeatedly formed and ruptured under alternative bias polarity.

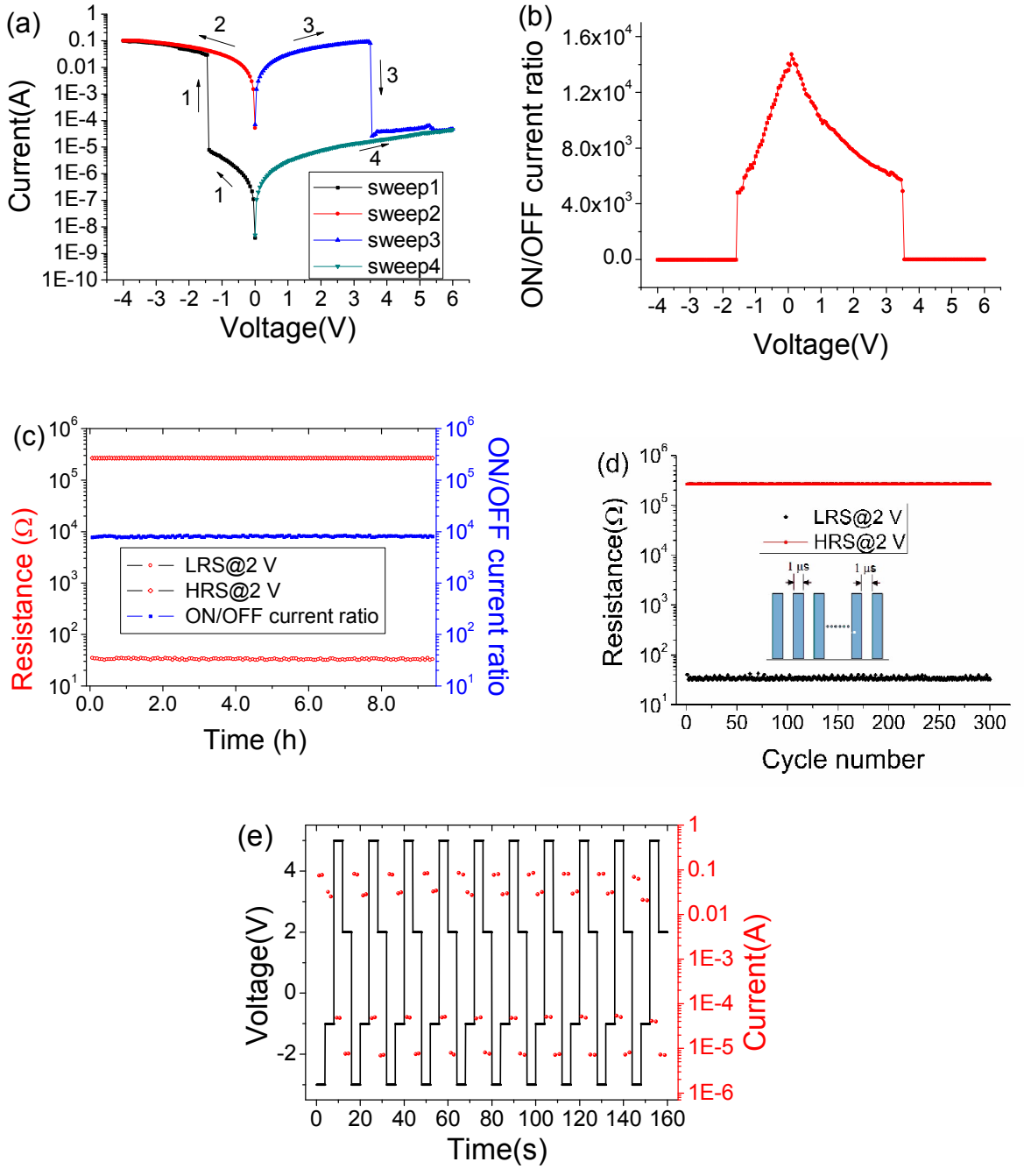

Fig. 3 (a) *I-V* characteristics of the blends films based memory devices with 5 wt.% PBD. (b) Relationship between the ON/OFF current ratio and the applied voltage of the devices with 5 wt.% PBD. (c) Stability of the

ITO/PVP+PBD/Al device with 5 wt. % PBD in either ON or OFF state under a constant stress of 2 V. (d) Effect of read cycles for the ON and OFF states in the above device. The inset shows the pulse shape in the measurement. (e) WRER cycles of the ITO/PVP+PBD/Al device with 5 wt. % PBD.

The device with 9 wt. % PBD also exhibits bistable electrical switching behavior, as illustrated by the *I-V* characteristics of Fig. 4(a). In the first voltage scan from 0 to -4 V, the current increases abruptly at a threshold voltage of about -1.6 V, indicating the transition from OFF state to ON state. The device remained in this ON state during the subsequent scan from 0 to -4 V (sweep 2). The distinct electrical bistable state in the voltage range of about 0 to -1.6 V, where the ON/OFF current ratio is more than 10^4, allowed a voltage of -0.8 V to read the "OFF" signal (before writing) and "ON" signal (after writing) of the memory device. In the subsequent positive voltage scan (sweep 3), the high conductivity state is maintained, thereby indicating the device with 9 wt. % PBD exhibits write-once-read-many times (WORM) memory behavior. It is both non-rewritable and nonvolatile after it has been turned on. Fig. 4(b) shows the retention times and stress tests of both the ON and OFF states of the device with 9 wt. % PBD. Initially, the memory devices started to turn ON or OFF to a high or low conductivity state. Under a constant stress of -0.8 V, no obvious increase in resistance (degradation in current) was observed for both ON and OFF states for 10.8 h during the test (Fig. 4(b)) and the memory devices were stable for at least 300 continuous read pulses of -0.8 V (Fig. 4(c).

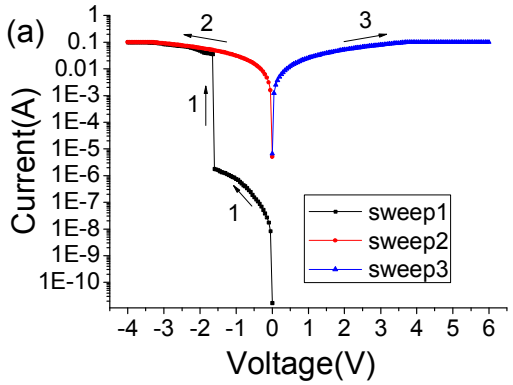

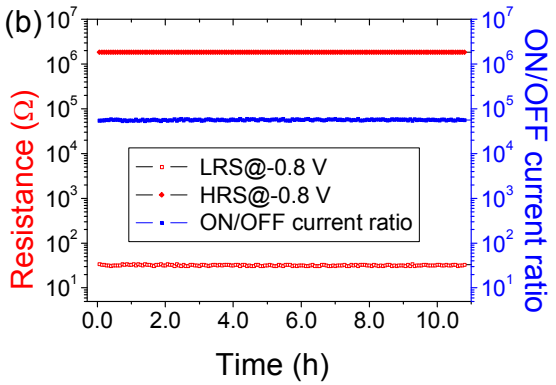

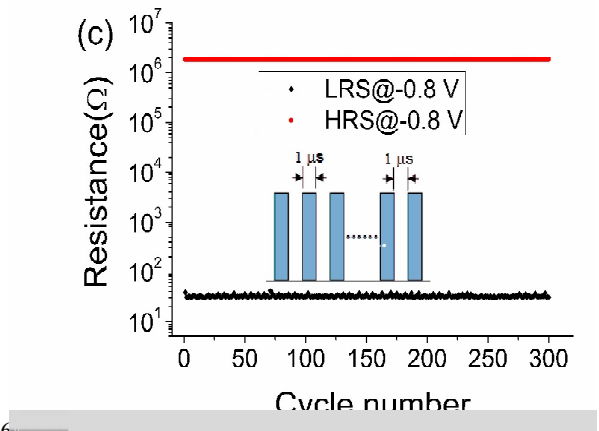

Fig. 4 (a) *I-V* characteristics of the blends films based memory devices with 9 wt. % PBD. (b) Stability of the ITO/PVP+PBD/Al device with 9 wt. % PBD in ON and OFF state under a constant stress at -0.8 V. (c) Effect of read cycles for the ON and OFF states in the above device. The inset shows the pulse shape in the measurement.

Further increase in PBD content of the composite film results in an insulator behavior, and the devices with 14 wt. % PBD exhibit a single low-conductivity state, and no conductance switching behavior is observed (Fig. 5).

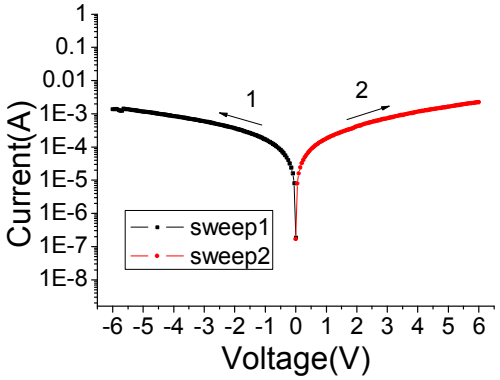

Fig. 5 *I-V* characteristics of the blends films based memory device with 14 wt. % PBD.

The cross-sectional view of the device consisting of the PVP +PBD composite, coated over a glass substrate before the evaporation of Al electrode is illustrated in Fig. 6. From the top to bottom is glass, ITO film and PVP+PBD composite film, respectively, the thickness of the different concentration of composite film can be judged as 134, 144, 142 and 139 nm from this image, respectively. The uniform distribution of the PBD in the PVP film is observed clearly from the image. The effect of PBD content in the composite films on device performance, including OFF state current, ON/OFF state current ratio, and turn-on voltage, is summarized in Fig. 7(a) and (b). The OFF state current of the composite films is decreased by 2 orders of magnitude with the increase in PBD content from 0 to 9 wt. %. As the content of PBD increased, the ON/OFF state current ratio of memory devices showed an increasing tendency. The turn-on voltage of the bistable devices also increase with increasing the content of PBD.

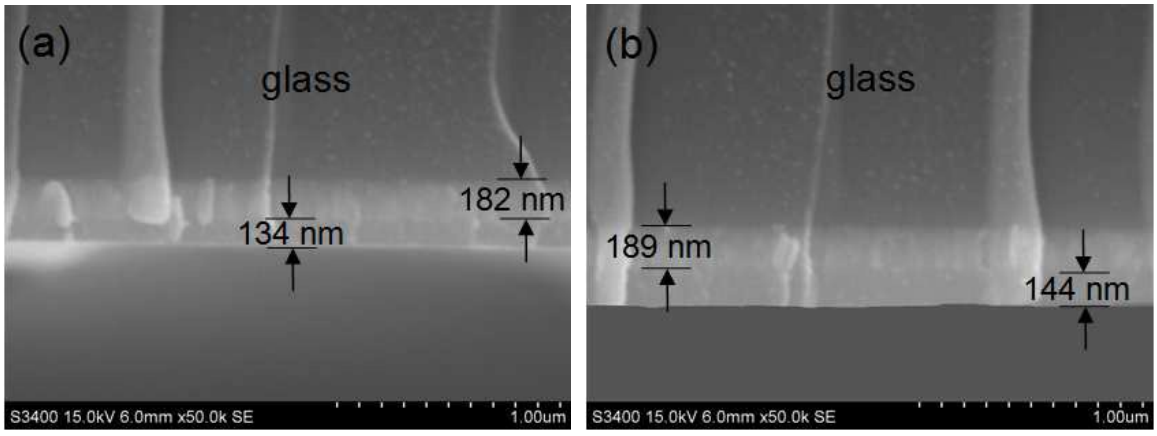

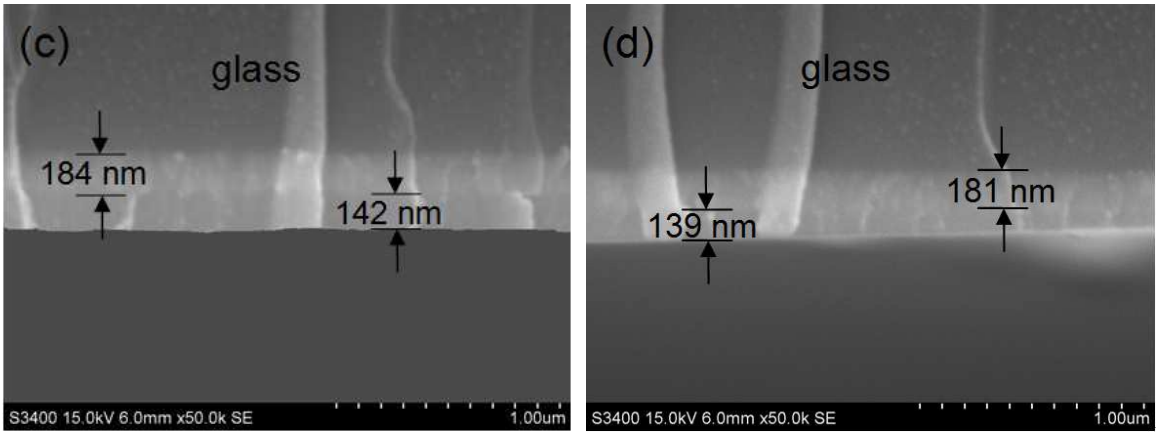

Fig. 6 Cross-section scanning electron microscopic images of the PVP+PBD composite film over a glass substrate with (a) 0 wt.% (b) 5 wt.% (c) 9 wt.% (d) 14 wt.% PBD loading.

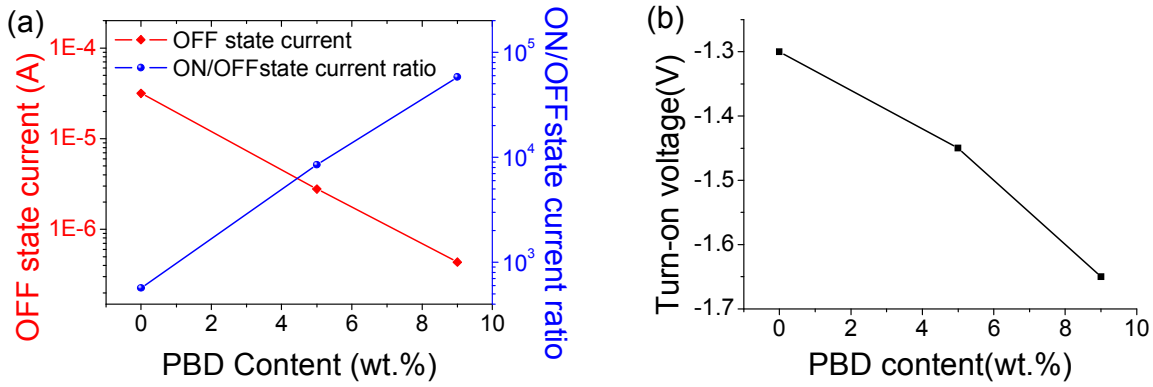

Fig. 7 (a) Effect of PBD content on the OFF state current and ON/OFF state current ratio of the devices when read at -0.8 V, (b) Effect of PBD content on turn-on voltage.

The memory properties of PVP+PBD composite film with different PBD content from 0 to 14 wt. % are summarized in Tab. 1. In general, the memory device reveals different electrical conductance behaviors from rewritable flash memory effect, WORM memory effect to insulator behavior with increasing the content of PBD.

Tab. 1 Memory properties of PVP+PBD composite film

PVP+PBD composite	0 wt. % PBD	5 wt. % PBD	9 wt. % PBD	14 wt. % PBD
memory property	rewritable flash	rewritable flash	WORM	insulator

Further information about the charge transport mechanism can be obtained from the *I-V* curves in ON and OFF states according to different theoretical models. Considering the low PBD content in the composites, PVP is the dominant component and acts as the matrix of the active layer in the present devices. In summary, PVP is an unstable dielectric material that contains deep traps originating from the enormous amount of -OH hydroxyl group that allows charging and decharging those traps upon applied voltage. This is a common phenomenon in PVP organic memory.[30] The ON state current of the bistable device can be fitted by Ohmic model, as shown in Fig. 8(a). For the OFF state of bistable devices, as shown in Fig. 8(b-d), in the lower applied voltage condition, the

slope of the log*I*-log*V* curve was calculated close to 1 (1.02, 1.08 and 1.03), which indicates that the conduction mechanism is dominated by Ohmic conduction. In the second and third region, the curve became steeper and the slope calculated was larger than 2. The observed carrier transportation characteristics are consistent with the trap-controlled space charge limited current (TC-SCLC) model.[31] The variation of the slope in the OFF state indicates that there are more charge traps after PBD was added into the PVP matrix. The introduced charge traps also reduced the current of low conductivity state.

To further understand the switching mechanism in the ITO/PVP+PBD/Al memory device, resistance was measured as a function of temperature in high and low conductivity state. As these organic materials cannot withstand high temperatures, the behavior of the resistances with temperature was measured in a window ranging from 293.5 to 373.5 K. Temperature dependence of resistance of the device in ON and OFF state is depicted in Fig. 8(e) and (f), the resistance of ON state increases with increasing the ambient temperature, indicating that they are in metallic states. However, the resistance of OFF state decreases with increasing the ambient temperature, implying a semiconducting character. This observation is consistent with the above discussion.

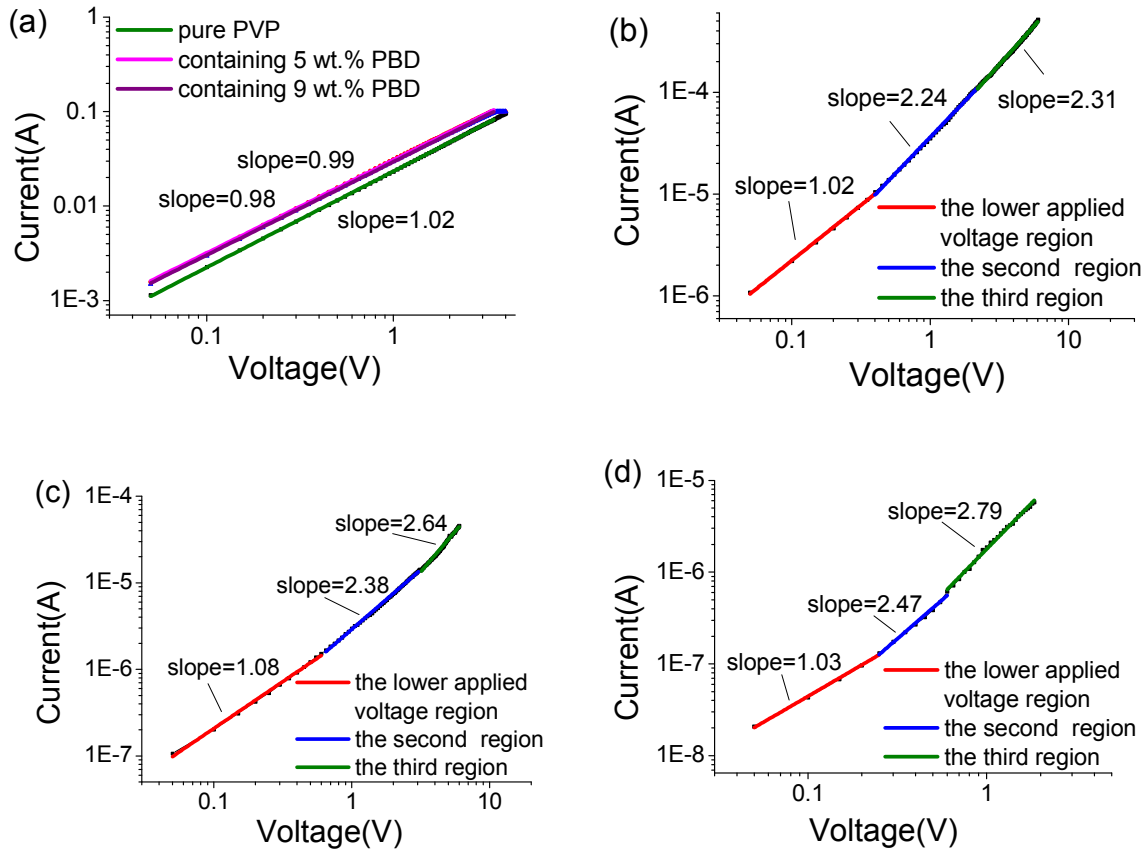

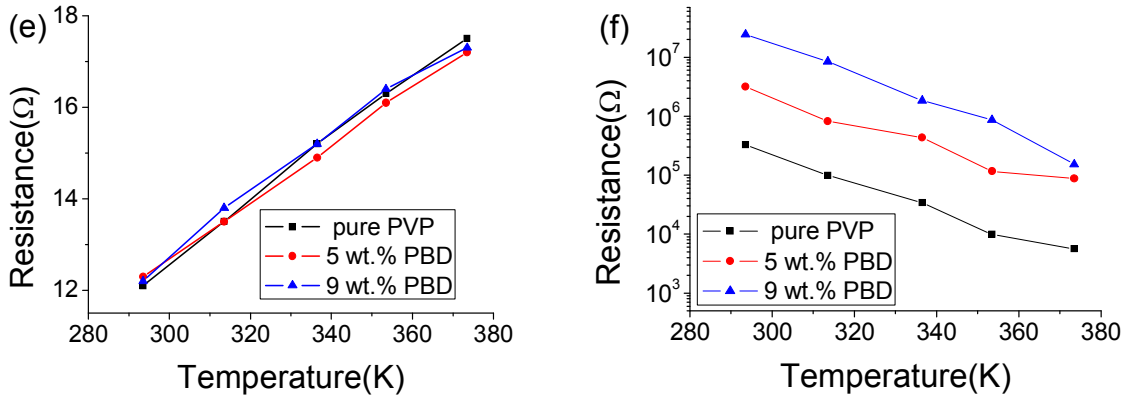

Fig. 8 Fitted *I-V* characteristics of the ITO/PVP+PBD/Al devices (a) ON state, (b) pure PVP (OFF state), (c) containing 5 wt. % PBD (OFF state), and (d) containing 9 wt. % PBD (OFF state), (e) Temperature dependence of the resistance of ON state. (f) Temperature dependence of the resistance of OFF state.

Fig. 9 shows the absorption spectra of different contents of PBD in the PVP solution. The intensities of the absorbance peak from pure PVP to containing 14 wt. % PBD are basically increased with the increasing of PBD content. It explains the possible guest additive-host matrix interaction associated with the charge-transfer-related switching mechanism.

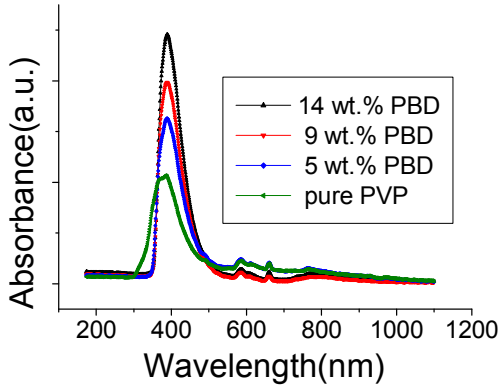

Fig. 9 Absorption spectra of PVP+PBD blend solution.

For ITO/PVP/Al device, upon applying a negative voltage to the top (Al) electrode, charge carriers are injected into the polymer film and trapped by PVP. The trapped electrons will induce a countering space charge layer in PVP near the Al electrode. The observed obvious resistive switching behavior should be related to the trapped and detrapped charge in the Schottky-like depletion layer.[32] Under low bias, charge carriers do not have sufficient energy/mobility to escape from trapping centers. At the threshold switching voltage, a majority of the charge trapping centers are filled, and a trap-free environment exists in PVP film. Percolation pathways for charge carriers are formed, switching the devices from the low conductivity state to high conductivity state. Due to the deep traps originating from the enormous amount of -OH hydroxyl group of PVP, charge

carriers are deeply trapped in hydroxyl group and stabilized by the PVP matrix. Upon application of a reverse (positive) bias of sufficient magnitude and with the elimination of the space-charge layer in PVP near the Al electrode interface, the trapped charges in the PVP will be neutralized or extracted. As a result, the device returns to the original OFF state, which is characteristic of a rewritable and nonvolatile memory device.

As the PVP+PBD blend thin film is activated by an electric field, the transferred charge is transported and delocalized effectively between two electrodes. Therefore, the PVP+PBD devices change from flash, WORM and eventually to insulator behavior in accordance with the PBD content. For the case of PVP+PBD blend with 9 wt. % PBD, the stable charge transfer environment makes charges hardly to recombine due to the high electron affinity of the PBD acceptors. The gradually increasing concentration of PBD consecutively leads to an enhanced electrical stability. The introduction of electronegative oxadiazole unit will lower the electron density in molecules and enhances their stabilities. As delocalized tunneling of field-induced charge transfer carriers occurs through the entire film, the nonvolatile flash/WORM memory behaviors are expected depending on the loading ratio of the PBD additives.

The experimental analysis suggests that the switching behavior is highly correlated to the loading ratio of guest additives in polymer host. The ability to restrain the back charge transfer is crucial to judge the flash/WORM behaviors. The present 5 wt. % PBD memory devices exhibit flash memory effect and the switching ON/OFF processes can be achieved by applying negative/positive voltage since recombination and transfer back of charges occur. This bipolar switching behavior indicates that switching effect has a close relationship on the applied electrical field. However, the nonerasable WORM memory effect in high concentration of PBD may arise from irreversible charge transfer.

The loss of PVP to some extent and charge traps induced by the PBD decreased the OFF state current. Because of the electron-withdrawing ability of PBD, electrons are deeply trapped by PBD and stabilized by the PVP matrix throughout the entire composite film. Thus, even after turning off the power supply, the PBD still retains the trapped charge carriers and the charged state. Consequently, the high conductivity (trap-filled) state remaines in the composite film, leading to the nonvolatile nature of the bistable device. Upon application of a reverse (positive) bias of sufficient magnitude and with the elimination of the space-charge layer in PVP near the organic matter/electrode interface, the trapped charges in the PBD will be neutralized or extracted. As a result, the device containing 5 wt. % PBD returns to the original less-conductive form and is programmed back to the OFF state, characteristic of the behavior of a rewritable flash memory.

For the device containing 9 wt. % PBD, the conformation of the phenyl ring with oxadiazole linkage of PBD is not a planar structure which may block the back charge transport occurring, and

also facilitates to stabilize the charge transport. Upon application of a reverse (positive) voltage scan to devices, the applied electric field is against by the build-in electric field associated with the space-charge layer in PVP. The build-in electric field can prevent the trapped electrons from being neutralized or extracted. Therefore, the devices remain in the high conductivity state and behave as a WORM memory.

4. Conclusion

In summary, we have developed an efficient and facile approach for accessing high performance organic semiconductor thin films via simply blending polymer and organic small molecules from the spin-coating process. The as-fabricated ITO/PVP+PBD/Al sandwich devices exhibit high ON/OFF current ratio that promises low misreading rate. The memory behaviors vary with the addition contents starting from nonvolatile flash and WORM memory to insulator behavior. These organic blend materials provide a viable way to become a memory controller in which a memory device has different types of memory therein (flash, WORM or insulator) through the loading ratio of guest additives.

Acknowledgements

The authors are grateful to the support of the National Science Foundation of China (Grant No. 61204127 and 11404180), the Natural Science Foundation of Heilongjiang Province, China (Grant No. A2015010).

Notes and references

1 B. Cho, S. Song, Y. Ji, T. W. Kim and T. Lee, *Adv. Funct. Mater.*, 2011, **21**, 2806.
2 W. Ren, Y. Zhu, J. Ge, X. Xu, R. Sun, N. Li, H. Li, Q. Xu, J. Zheng and J. Lu, *Phys. Chem. Chem. Phys*., 2013, **15**, 9212.
3 S. Song, B. Cho, T. W. Kim, Y. Ji, M. Jo, G. Wang, M. Choe, Y. H. Kahng, H. Hwang and T. Lee, *Adv. Mater*., 2010, **22**, 5048.
4 C. L. Liu and W. C. Chen, *Polym. Chem*. 2011, **2**, 2169.
5 A. D. Yu, T. Kurosawa, Y. H. Chou, K. Aoyagi, Y. Shoji, T. Higashihara, M. Ueda, C. L. Liu and W. C. Chen, *ACS Appl. Mater. Interfaces*, 2013, **5**, 4921.
6 C. J. Chen, Y. C. Hu and G. S. Liou, *Chem. Commun*., 2013, **49**, 2804.
7 C. D. Rosa, F. Auriemma, R. D. Girolamo, G. P. Pepe, T. Napolitano and R. Scaldaferri, *Adv. Mater*., 2010, **22**, 5414.
8 C. O. Baker, B. Shedd, R. J. Tseng, A. A. Martinez-Morales, C. S. Ozkan, M. Ozkan, Y. Yang and R. B. Kaner, *ACS Nano*, 2011, **5**, 3469.
9 M. A. Mamo, A. O. Sustaita, N. J. Coville and I. V. Hummelgen, *Org. Electron.*, 2013, **14**, 175.
10 Q. Zhang, J. Pan, X. Yi, L. Li and S. Shang, *Org. Electron*., 2012, **13**, 1289.
11 A. -D. Yu, C. -L. Liu and W. -C. Chen, *Chem. Commun*., 2012, **48**, 383.
12 Y. Ji, S. Lee, B. Cho, S. Song and T. Lee, *ACS Nano*, 2011, **5**, 5995.
13 G. Liu, Q. -D. Ling, E. Y. H. Teo, C.-X. Zhu, S. -H. Chan, K.-G. Neoh and E.-T. Kang, *ACS*

Nano, 2009, **3**, 1929.

14 S. ChandraKishore and A. Pandurangan, *RSC Adv.*, 2014, **4**, 9905.

15 K. K. Park, J. H. Jung and T. W. Kim, *Appl. Phys. Lett.*, 2011, **98**, 193301.

16 J. Huang and D. Ma, *Appl. Phys. Lett.*, 2014, **105**, 093303.

17 T. Suga, S. Takeuchi and H. Nishide, *Adv. Mater.*, 2011, **23**, 5545.

18 R. Sim, W. Ming, Y. Setiawan and P. S. Lee, *J. Phys. Chem. C*, 2013, **117**, 677.

19 I. Salaoru and S. Paul, *Thin Solid Films*, 2010, **519**, 559.

20 Y. -K. Fang, C. -L. Liu and W. -C. Chen, *J. Mater. Chem.*, 2011, **21**, 4778.

21 L. Pan, B. Hu, X. Zhu, X. Chen, J. Shang, H. Tan, W. Xue, Y. Zhu, G. Liu and R. W. Li, *J. Mater. Chem. C*, 2013, **1**, 4556.

22 K. L. Wang, Y. L. Liu, J. W. Lee, K. G. Neoh and E. T. Kang, *Macromolecules*, 2010, **43**, 7159.

23 X. Wang, S. Guan, H. Xu, X. Su, X. Zhu and C. Li, *J. Polym. Sci. Pol. Chem.*, 2010, **48**, 1406.

24 K. Tsuchiya, K. Sakaguchi, H. Kasuga, A. Kawakami, H. Taka, H. Kita and K. Ogino, *Polymer*, 2010, **51**, 616.

25 W. Kwon, B. Ahn, D. M. Kim, Y. -G. Ko, S. G. Hahm, Y. Kim, H. Kim and M. Ree, *J. Phys. Chem. C*, 2011, **115**, 19355.

26 K. Kim, Y. K. Fang, W. Kwon, S. Pyo, W. C. Chen and M. Ree, *J. Mater. Chem. C*, 2013, **1**, 4858.

27 J. Bettenhausen and P. Strohriegl, *J. Appl. Phys.,* 1997, **82**, 4957.

28 Y. M. Sun, L. Li, D. Z. Wen and X. D. Bai, *Org. Electron.*, 2015, **25**, 283.

29 Y. M. Sun, L. Li, D. Z. Wen and X. D. Bai, *J. Phys. Chem. C*, 2015, 119,19520.

30 C. C. Chang, Z. Pei and Y. J. Chan, *Appl. Phys. Lett.*, 2008, **93**, 143302.

31 Y. C. Chen, H. C. Yu, C. Y. Huang, W. L. Chung, S. L. Wu and Y. K. Su, *Sci. Rep.*, 2015, DOI: 10.1038/srep10022.

32 B. Sun, C. M. Li, Phys. *Phys. Chem. Chem. Phys.*, 2015, **17**, 6718.